



Published in final edited form as:

J Phys Chem B. 2005 March 03; 109(8): 3157–3162. doi:10.1021/jp045186t.

Fast and Slow Deposition of Silver Nanorods on Planar Surfaces: Application to Metal-Enhanced Fluorescence

Kadir Aslan[†], Zoya Leonenko[‡], Joseph R. Lakowicz[‡], Chris D. Geddes^{*†‡}

Institute of Fluorescence, Laboratory for AdVanced Medical Plasmonics, Medical Biotechnology Center, University of Maryland Biotechnology Institute, and Center for Fluorescence Spectroscopy, Department of Biochemistry and Molecular Biology, Medical Biotechnology Center, University of Maryland School of Medicine, 725 West Lombard Street, Baltimore, Maryland 21201

Abstract

Two methods have been considered for the deposition of silver nanorods onto conventional glass substrates. In the first method, silver nanorods were deposited onto 3-(aminopropyl)triethoxysilane-coated glass substrates simply by immersing the substrates into the silver nanorod solution. In the second method, spherical silver seeds that were chemically attached to the surface were subsequently converted and grown into silver nanorods in the presence of a cationic surfactant and silver ions. The size of the silver nanorods was controlled by sequential immersion of silver seed-coated glass substrates into a growth solution and by the duration of immersion, ranging from tens of nanometers to a few micrometers. Atomic force microscopy and optical density measurements were used to characterize the silver nanorods deposited onto the surface of the glass substrates. The application of these new surfaces is for metal-enhanced fluorescence (MEF), whereby the close proximity of silver nanostructures can alter the radiative decay rate of fluorophores, producing enhanced signal intensities and an increased fluorophore photostability. In this paper, it is indeed shown that irregularly shaped silver nanorod-coated surfaces are much better MEF surfaces as compared to traditional silver island or colloid films. Subsequently, these new silver nanorod preparation procedures are likely to find a common place in MEF, as they are a quicker and much cheaper alternative as compared to surfaces fabricated by traditional nanolithographic techniques.

1. Introduction

Synthesis of anisotropic metal nanoparticles has been the subject of many scientific reports in recent years in consideration for applications in nanoscience and nanotechnology.^{1–19} Several solution preparation methods have been devised for silver nanorods,^{2–6} silver triangular nanoplates,^{7–8} triangles,^{9–13} silver nanowires,¹⁴ and gold nanorods^{15–19} in solution. Examples of these methods include surfactant-based seed-mediated growth,^{2,7,8,15–19} thermal growth,^{9–11} and photoreduction processes.¹²

*To whom correspondence should be addressed. geddes@umbi.umd.edu.

[†]University of Maryland Biotechnology Institute.

[‡]University of Maryland School of Medicine.

In contrast, the assembly of anisotropic metal nanoparticles on planar surfaces still requires more sophisticated methods such as lithography. One of the more notable examples is “nanosphere lithography (NSL)” developed by Van Duyne and co-workers.^{20,21} Although NSL is a reliable technique to produce well-defined anisotropic silver nanoparticles on solid substrates, it is an expensive and somewhat tedious technology. Recently, Taub et al.²² reported the growth of gold nanorods directly on mica using a method based on the solution-seeded nanorod synthesis scheme.¹⁹ This technique was introduced as a first step toward removing the need for wet-chemical lithographic processes. In addition, Wei et al.²³ extended this method for gold nanorods to conventional glass substrates.

In this work, the deposition of silver nanorods on conventional glass substrates, analogous to the wet-chemical method that was applied for the growth of gold nanorods on mica, is reported. This new approach enables one to control the size/loading density of the silver nanorods on the glass substrates by controlling simple experimental parameters such as immersion time, concentration, temperature, and the surfactant. These advances are directed at fabricating new quick and cheap silvered surfaces for applications in metal-enhanced fluorescence.^{25–28}

Over the past several years the laboratories at the University of Maryland at Baltimore and University of Maryland Biotechnology Institute have shown the favorable effects that can be obtained for fluorophores in close proximity to metallic surfaces, such as enhanced quantum yields, increased excitation rates, and an increased fluorophore photostability.^{25–28} These experimental platforms have widely utilized both silver island films²⁸ and silver colloid films,²⁸ and have typically resulted in fluorescence intensity enhancements of 5–30-fold.²⁸ However, silver fractal-like surfaces, which were grown by passing a current between silver electrodes in deionized water,²⁸ have produced localized enhancements of several-thousand-fold, which was also predicted by theory some time ago.²⁵ Most of the efforts have focused on producing rodlike structures on surfaces which possess characteristics similar to those of the fractals with regard to shape and size,²⁸ but use simple chemistries and no electric currents in their preparation. Similar to fractals, the rods are not ordered but are in fact highly irregular, producing typical enhancements in indocyanine green fluorescence of ~50-fold. These new novel surfaces could find a common place in applications of MEF and replace the traditional silver island film MEF platforms.

2. Materials and Methods

2.1. Materials.

Silver nitrate (99.9%), sodium citrate (99%), L-ascorbic acid (99%), sodium borohydride (98%), 3-(aminopropyl)triethoxysilane (APS), sodium hydroxide (99.996%), and cetyltrimethylammonium bromide (CTAB; 99%) were obtained from Sigma-Aldrich. All chemicals were used as received. Premium quality glass slides were purchased from Fisher Scientific (75 × 25 mm).

2.2. Methods.

2.2.1. Synthesis of Silver Nanorods in Solution.—The preparation of silver nanorods *in solution* is performed by using the procedure published by Murphy and co-workers.² First, silver seeds were prepared in solution: silver nitrate was reduced by sodium borohydride in the presence of sodium citrate to produce 4 ± 2 nm silver nanoparticles.² The silver nanorods were grown in solution by injecting a solution of silver seeds into growth medium that contains silver nitrate, ascorbic acid, and CTAB. To accelerate the nanorod growth, NaOH is added to the growth solution. The solution was initially clear and changed to a green color after the reaction was complete.

2.2.2. Preparation of Glass Substrates.—Glass slides were cleaned with “piranha solution” for at least 2 h (3:7 30% hydrogen peroxide/concentrated sulfuric acid) *Caution: Piranha solution reacts violently with most organic materials and should be handled with extreme care!* Then, the glass substrates were rinsed extensively with deionized water and dried in a stream of dry nitrogen prior to use. The cleaned slides were silanized by immersing them in a 2% ethanolic solution of APS for 2 h. Then, the APS-coated glass slides were rinsed in ethanol and water, and sonicated in ethanol for 30 s. Finally, the APS-coated slides were rinsed with water and dried with a stream of nitrogen gas.

2.2.3. Slow Deposition of Silver Nanorods onto Glass Substrates.—The silver nanorods were deposited onto the APS-coated glass slides by simply immersing the slides in the silver nanorod solution at room temperature. The optical density of the silvered slides depends on the immersion time and the concentration of the silver nanorods.

2.2.4. Rapid Deposition of Silver Nanorods onto Glass Substrates.—The APS-coated glass slides were immersed in the silver seed solution for ~30 min, rinsed with deionized water, and then dried in a stream of nitrogen gas. The silver seed-coated glass slides were then immersed in 40 mL of 0.80 M CTAB solution for 5 min. A 1 mL sample of 10 mM AgNO₃ and 2 mL of ascorbic acid were then added. A 0.4 mL sample of 1 M NaOH was immediately added, and the solution was mixed gently to accelerate the growth process. The silver nanorods were formed on the glass slides within 10 min evident by the color change (clear to green) on the glass slide and in the solution. To increase the loading of silver nanorods on the surface, the silver nanorod-coated glass substrates were immersed in CTAB again, similar amounts of AgNO₃, ascorbic acid, and NaOH being added as in the first step. This process can be repeated until the desired loading of the silver nanorods onto the glass slides is obtained (Figure 1).

All absorption measurements were performed using an HP 8453 UV-vis spectrophotometer. AFM images were collected with an atomic force microscope (TMX 2100 Explorer SPM, Veeco) equipped with an AFM dry scanner (the scanning area was 100 × 100 nm). The surfaces were imaged in air, in a tapping mode of operation, using SFM non-contact-mode cantilevers (Veeco). Samples were freshly prepared prior to imaging. The AFM scanner was calibrated using a standard calibration grid as well as by using gold nanoparticles, 100 nm in diameter, from Ted Pella. The images were analyzed using SPMLab software.

2.2.5. Coating of Fluorophore–Protein onto Silver Nanorod Surfaces.—In this work, the long-wavelength dye indocyanine green (ICG), which is widely used in a variety of in vivo medical applications, is utilized.³⁴ ICG is not toxic and is approved by the U.S. Food and Drug Administration for use in humans, typically by injection. ICG displays a low quantum yield in solution, ~ 0.016 ,³⁵ making it a good candidate for MEF, since low-quantum-yield fluorophores result in greater enhancements.²⁵ Binding the ICG-HSA (ICG is noncovalently bound to HSA) to the silver nanorod-deposited glass slides was accomplished by soaking in a $30 \mu\text{M}$ ICG, $60 \mu\text{M}$ HSA solution for 2 h, followed by rinsing with water to remove the unbound material. Both the glass and silver nanorod-deposited surfaces were coated with the labeled HSA, which is known to passively adsorb to noble metal surfaces and form a ~ 4 nm thick protein monolayer, allowing one to study the fluorescence spectral properties of noncovalent ICG-HSA complexes in the absence and presence of silver nanorods. By equally coating a glass microscope slide with ICG-HSA, the enhancement factor (benefit) obtained from using the silver was determined, i.e., intensity on silver/intensity on glass, given that both surfaces are known to have almost equal monolayer coverages.³⁰ The experimental setup used to observe the emission from both silvered and unsilvered slides has been reported by the authors previously.^{28,29}

3. Results and Discussion

The silver nanorods were deposited onto glass substrates by two deposition methods, namely, by slow and rapid deposition. Silver nanorods in solution, which were deposited on glass slides simply by APS adsorption (denoted as the slow deposition method), were prepared by the seed-mediated method in the presence of CTAB as published previously by Murphy and co-workers.² The characterization of these silver nanorods was done by using transmission electron microscopy (TEM) and optical density measurements. Figure 2 (top) shows a typical TEM image of the silver nanorods prepared in solution. TEM reveals that the silver nanorods have an approximate average aspect ratio (length/width = 50×25 nm) of 2 (Figure 2, top). Silver nanorods in solution have two distinct surface plasmon peaks: 440 and 550 nm (Figure 2, bottom). The surface plasmon peak at 440 nm is the transverse plasmon peak, and the peak at 550 nm is the longitudinal plasmon peak. The wavelength where the longitudinal plasmon peak appears is dependent on the length of the silver nanorods, that is, the longer the nanorod, the greater the red-shifted peak appears.² Typical optical density value for the longitudinal plasmon peak of the silver nanorods prepared in this work was approximately 1.0.

The simple adsorption of the silver nanorods to the glass slides from the solution took several days to complete, where the absorption at 550 nm reached only 20% that of the silver nanorods in solution. Surprisingly, immersion of glass slides for even longer times did not result in a further increase in this value, which is in contrast to the results for silver colloids immobilized on glass surfaces reported previously.²⁴ Additionally, a red shift in this band to longer wavelengths was observed. The observations described above are influenced by two factors: (1) interactions of CTAB with the amine-terminated silane on the glass surface and (2) the repetitive heating of the silver nanorod solution while the glass slides are immersed (for 15 min at 40°C), to maintain the shape of the silver nanorods. CTAB was not removed from the silver nanorod solution, and since CTAB crystallizes while the glass slides are

immersed after a period of time, the silver nanorod solution had to be heated to *redissolve* CTAB crystals.

Since both CTAB and amine-terminated silane (on the glass slide) carry positive charges at the experimental conditions employed (see the Materials and Methods), the adsorption of CTAB-coated silver nanorods onto APS-coated glass slides is hypothesized to be very slow due to the electrostatic forces, taking a very long time to complete. Given that CTAB crystallizes over time (every 10 h) while the glass slide is immersed (at room temperature), the solution was therefore heated (40 °C) many times during the deposition process. The repetitive heating of the silver nanorod solution is speculated to play an important role in the reorganization of CTAB-coated silver nanorods in solution, and subsequently those that were deposited onto the glass surface, where the micellar forms of CTAB-containing silver nanorods changed shape during crystallization and reorganization after each heating cycle. The evidence for this is provided in Figure 3. Figure 3 shows the absorption spectra of silver nanorods in the growth medium before and after continuous heating at 40 °C for 48 h. The continuous heating of CTAB-coated silver nanorods results in conversion of the nanorod shape to spheres. It is therefore concluded that the intermittent heating of the solution of CTAB-coated silver nanorods while the glass slide is immersed results in a slower deposition of silver nanorods onto the surface. The observed broadening of the longitudinal resonance peak is also a result of the reorganization of the silver nanorods on the surface; that is, silver nanorods aggregated, and/or longer nanorods are formed.

In view of the fact that the deposition of silver nanorods onto glass slides from solution is time-consuming and is proven to be problematic (shape change due to crystallization/reheating of CTAB), another method was devised, where the silver nanorods are directly grown on the glass substrate as outlined in Figure 1. In this procedure, the preadsorbed small-sized silver spheres in conjunction with CTAB and silver ions mediate the rapid growth of silver nanorods directly on the glass slides.

Sequential growth experiments, in which the growth process (repeated several times) was monitored by atomic force microscopy and absorption spectroscopy, were conducted. Figure 4 (top) shows a typical AFM image of the silver nanorods that are grown on APS-coated glass slides with low loading density. The loading density of silver nanorods was controlled by the time that the glass slides were kept in the CTAB solution after the silver ions/ascorbic acid and NaOH (used for speeding up the reactions) were added. The AFM image in Figure 4 (top) is obtained after 5 min of incubation of the glass slides in the reaction mixture after NaOH was added. Figure 4 (top) also reveals that all the silver particles were grown substantially and approximately 10% of the particles were indeed nanorods. The aspect ratio of the silver nanorods was larger than 2 with a length in the range of 100–300 nm and a diameter of 10–40 nm (height in the AFM image).

The loading density and the size of the silver nanorods were further increased by incubating the glass slides, with low-loading-density silver nanorods, in a fresh CTAB solution and adding silver ions and ascorbic acid after 5 min, similar to the procedure applied by Taub et al.,²² and the sequential growth process also used by Murphy and co-workers for the growth of longer silver nanorods in solution.² Figure 4 (bottom) shows a typical AFM image of the

silver nanorods that are grown on APS-coated glass slides with a high loading density. After three subsequent growth stages all the silver particles were converted to silver nanorods. The aspect ratio of the silver nanorods was much larger than 2 (up to 10) with a length ranging from a few hundred nanometers to a few micrometers, and a diameter ranging from a few hundred nanometers to a few micrometers (height in the AFM image). Figure 5 shows the progressive increase in the absorption of the silver nanorods that were grown from the silver seeds. It is noted that the transverse plasmon peak is more dominant in the beginning of the growth process; however, as longer nanorods are formed the longitudinal plasmon absorption peak becomes, as expected, more dominant.

It is well-known that the positively charged amine groups have affinity for the negatively charged silver nanoparticles. Thus, the silver seeds (4 nm) are chemically attached to the surface (Figure 5). After the incubation of silver seed-coated glass slides in CTAB, and the addition of more silver ions to the mixture, silver seeds are readily converted into silver nanorods. It was found that CTAB should be allowed to adsorb on the surface for longer than 1 min prior to the addition of silver ions and the ascorbic acid to obtain a relatively high nanorod yield, but not longer than 10 min, after which time the nanorods were unable to grow at all. Similar observations were also made for the growth of gold nanorods on mica surfaces by Taub et al.²² According to their findings, most of the nanorod growth occurred within 10 min after the addition of gold salt and ascorbic acid to the CTAB solution.

Although the surface growth technique employed in this work is analogous to the solution growth process, several differences exist as also discussed by Taub et al.²² for the growth of gold nanorods on mica surfaces: (1) the amount of seed particles on the glass slides is significantly less than that used in the solution growth process, (2) the growth of silver nanorods on the surface is not controlled by the diffusion of seed particles but rather is effected by the interactions of CTAB with the surface and the diffusion of silver ions that were added later. The amount of silver seeds that can adsorb onto the APS-coated glass slide is controlled by the incubation time of the glass slides in the silver seed solution. It was discovered that the incubation of silver seeds for longer than 30 min did not result in an effective growth of the silver nanorods. This is explained by the following: as more silver seeds are allowed to adsorb onto the surface (that is, the surface coverage of silver seeds increases), there is a significant reduction in the size of the micellar structures and the amount of CTAB that can adsorb onto the glass slide, since CTAB preferentially adsorbs onto the negatively charged silver seeds. Thus, it is hypothesized that CTAB micelles mediate the nanorod formation on the surface of the glass slide, and a reduction in the size/amount of these micelles results in the reduction of the efficiency of the growth process. In addition, the growth of silver nanorods is terminated by the accumulation of multilayers of CTAB on the surface around the growing particles, blocking the access of silver ions to the growing nanorods.

In the growth process employed here, there is a significant amount of silver ions in the reaction mixture, some of which are converted to silver nanorods in solution even after the growth on the surface is completed. This was confirmed by the observations that the growth solution changed color from clear to light green during the growth process. This could be explained by the detachment of the loosely bound silver seeds from the surface and/or the

incomplete rinsing step after the incubation of APS-coated slides in the silver seed solution. As suggested by Taub et al.²² for the growth of gold nanorods on mica, the presence of a large excess of metal ions in the reaction mixture is also verified by the length of the nanorods formed being longer than that of the nanorods obtained in a single step of the solution growth process.

3.1. Application of These Substrates to Metal-Enhanced Fluorescence.

To the best of the authors' knowledge, this is the first report of the rapid growth of silver nanorods on conventional substrates. In recent years the laboratories at the University of Maryland at Baltimore and University of Maryland Biotechnology Institute have reported favorable effects for fluorophores conjugated to proteins placed in close proximity to surface-immobilized silver nanostructures (greater quantum yields, reduced lifetimes, and/or increased photostability).^{25–32} This experimental format has been adopted for two main reasons, the first being that the protein coverage with human serum albumin (HSA) is known to bind to silvered surfaces and indeed forms a monolayer³⁰ and the second being that the dimensions of the protein are such that the protein allows for a mean separation of the silver and the fluorophore, MEF being a through-space phenomenon, as demonstrated by the late T. Cotton.³³ In contrast, surface-enhanced Raman scattering (SERS) is known to be a consequence of contact between the species of interest (fluorophore) and the silvered surface.³³

To test the usefulness of the new substrates with regard to MEF, the substrates were subsequently coated with ICG-HSA as described in section 2.2.5 and shown in Figure 6. For a low loading of the nanorods on the surface ($A_{650} = 0.10$) a typical fluorescence enhancement of 10 can be obtained. However, for higher loadings, ($A_{650} = 0.48$), reproducible enhancements of 50-fold and even greater can be achieved, Figure 6, top. Figure 6, bottom, also shows that the spectral characteristics of ICG are maintained, as previously observed with silver island films also.³⁰ In these geometries, a typical 20-fold enhancement is achieved for ICG.³⁰ This strongly suggests the use of these new surfaces for routine applications in MEF.

With regard to the emerging use of MEF in sensing applications,^{28–32} the method and protocols presented here could be a useful tool for the simpler production of silver assay platforms that can be utilized in biotechnological applications such as high-throughput screening and drug discovery based on enhanced fluorescence detection.^{28–32} Silver nanorods that are grown on glass substrates could significantly improve the sensitivity of fluorescence-based biological assays, as compared to both surfaces comprised of silver island films and, indeed, unsilvered surfaces. Further studies by the authors are under way and will be reported in due course.

4. Conclusions

A simple and rapid wet-chemical technique for the deposition of silver nanorods on conventional glass substrates, which alleviates the need for lithography, is developed. The technique is based on the seed-mediated CTAB-directed growth of silver nanorods on glass surfaces. Silver nanorods prepared in solution were also deposited onto the glass substrates

for comparison. While it took several days to deposit silver nanorods from solution, the rapid deposition technique significantly reduced the deposition time to several hours. AFM studies revealed that the size of the silver nanorods varied from a hundred nanometers to a few micrometers. Interestingly, these new surfaces are a significant improvement over silver island films for applications in metal-enhanced fluorescence, with routine 50-fold enhancement in emission intensity typically observed for protein-immobilized indocyanine green.

Acknowledgment.

This work was supported by NIH Grant GM070929. Partial salary support to C.D.G. and J.R.L. from UMBI is also acknowledged.

Glossary

AFM	atomic force microscopy
APS	3-(aminopropyl)triethoxysilane
CTAB	cetyltrimethylammonium bromide
ICG	indocyanine green
MEF	metal-enhanced fluorescence
RDE	radiative decay engineering
TEM	transmission electron microscopy

References and Notes

- (1). Xia Y; Yang P; Sun Y; Wu Y; Mayers B; Gates B; Yin Y; Kim F; Yan H *Adv. Mater* 2003, 15, 353.
- (2). Jana NR; Gearheart L; Murphy CJ *Chem. Commun* 2001, 7, 617.
- (3). Zhu JJ; Liao XH; Zhao XN *Mater Lett.* 2001, 49, 91.
- (4). Xiong YJ; Xie Y; Du GO *Chem. Lett* 2002, 1, 98.
- (5). Hu JQ; Chen Q; Xie ZX *Adv. Funct. Mater* 2004, 14, 183.
- (6). Chen DL; Gao LJ *Cryst. Growth* 2004, 264, 216–222.
- (7). Chen SH; Fan ZY; Carroll DL *J. Phys. Chem. B* 2002, 106, 10777.
- (8). Chen SH; Carroll DL *Nano Lett.* 2002, 2, 1003.
- (9). Sun Y; Mayers B; Xia Y *Nano Lett.* 2003, 3, 675.
- (10). Jin R; Cao C; Hao E; Metraux GS; Schatz GC; Mirkin CA *Nature* 2003, 42, 487.
- (11). Callegari A; Tonti D; Chergi MP *Nano Lett.* 2003, 3, 1565.
- (12). Maillard M; Huang P; Brus L *Nano Lett.* 2003, 3, 1611.
- (13). Junior AM; de Oliveria HPI; Gehlen MH *Photochem. Photobiol. Sci* 2003, 2, 921. [PubMed: 14560809]
- (14). Caswell KK; Bender CM; Murphy CJ *Nano Lett.* 2003, 3, 677.
- (15). Jana NR; Gearheart L; Murphy CJ *Adv. Mater* 2001, 13, 1389.
- (16). Jana NR; Gearheart L; Murphy CJ *Chem. Mater* 2001, 13, 2313.
- (17). Murphy CJ; Jana NR *Adv. Mater* 2002, 14, 80.
- (18). Jana NR; Gearheart L; Obare SO; Murphy CJ *Langmuir* 2002, 18, 922.
- (19). Jana NR; Gearheart L; Murphy CJ *J. Phys. Chem. B* 2001, 105, 4065.

- (20). Haynes CL; McFarland AD; Zhao LL; Van Duyne RP; Schatz GC; Gunnarsson L; Prikulis J; Kasemo B; Kall MJ *Phys. Chem. B* 2003, 107, 7337.
- (21). Haynes CL; Van Duyne RP *Nano Lett.* 2003, 3, 939.
- (22). Taub N; Krichevski O; Markovich GJ *Phys. Chem. B* 2003, 107, 11579.
- (23). Wei Z; Mieszawska AJ; Zamborini FP *Langmuir* 2004, 20, 4322. [PubMed: 15969133]
- (24). Geddes CD; Cao H; Gryczynski I; Gryczynski Z; Fang J; Lakowicz JR *J. Phys. Chem. A* 2003, 107, 3443.
- (25). Lakowicz JR *Anal. Biochem* 2001, 298, 1. [PubMed: 11673890]
- (26). Lakowicz JR; Shen Y; D'Auria S; Malicka J; Fang J; Gryczynski Z; Gryczynski I *Anal. Biochem* 2002, 301, 261. [PubMed: 11814297]
- (27). Geddes CD; Lakowicz JR *J. Fluoresc* 2002, 12, 121.
- (28). Geddes CD; Aslan K; Gryczynski I; Malicka J; Lakowicz JR In *ReV. Fluoresc* 2004, 365 and references therein.
- (29). Lakowicz JR; Geddes CD; Gryczynski I; Malicka J; Gryczynski Z; Aslan K; Lukomska J; Matveeva E; Zhang J; Badugu R; Huang JJ *Fluoresc.* 2004, 14 (4), 425.
- (30). Malicka J; Gryczynski I; Geddes CD; Lakowicz JR *J. Biomed. Opt* 2003, 8 (3), 472. [PubMed: 12880353]
- (31). Gryczynski I; Malicka J; Geddes CD; Lakowicz JR *J. Fluoresc* 2003, 12, 11.
- (32). Geddes CD; Parfenov A; Roll D; Fang J; Lakowicz JR *Langmuir* 2003, 19, 6236. [PubMed: 20725608]
- (33). Sokolov K; Chumanov G; Cotton TM *Anal. Chem* 1998, 70, 3898–3905. [PubMed: 9751028]
- (34). Schutt F; Fischer J; Kopitz J; Holz FG *Clin. Exp. Invest* 2002, 30 (2), 110.
- (35). Sevick-Muraca EM; Lopez G; Reynolds JS; Troy TL; Hutchinson CL *Photochem. Photobiol* 1997, 66, 55. [PubMed: 9230705]

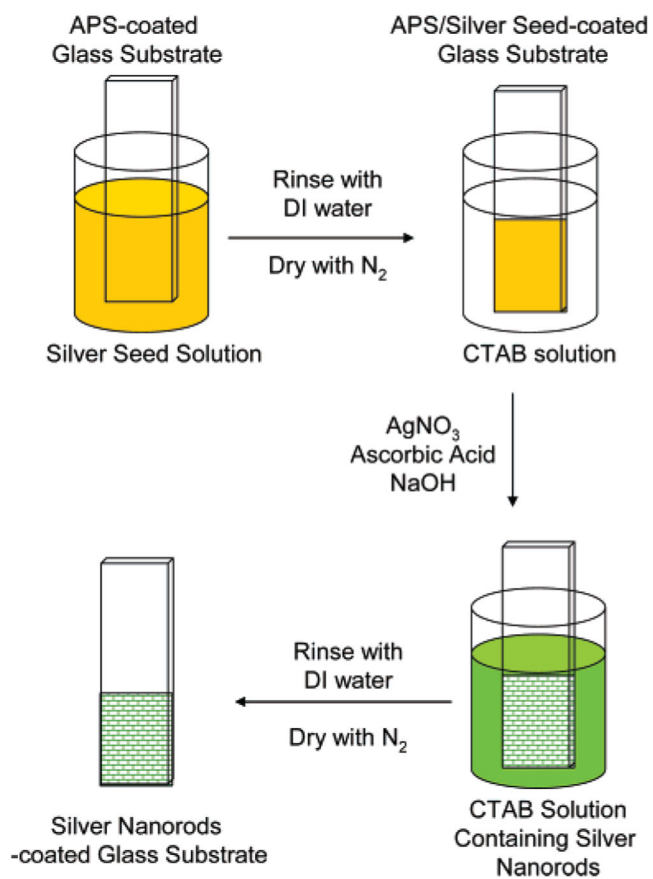


Figure 1.
Rapid deposition of silver nanorods on a glass substrate.

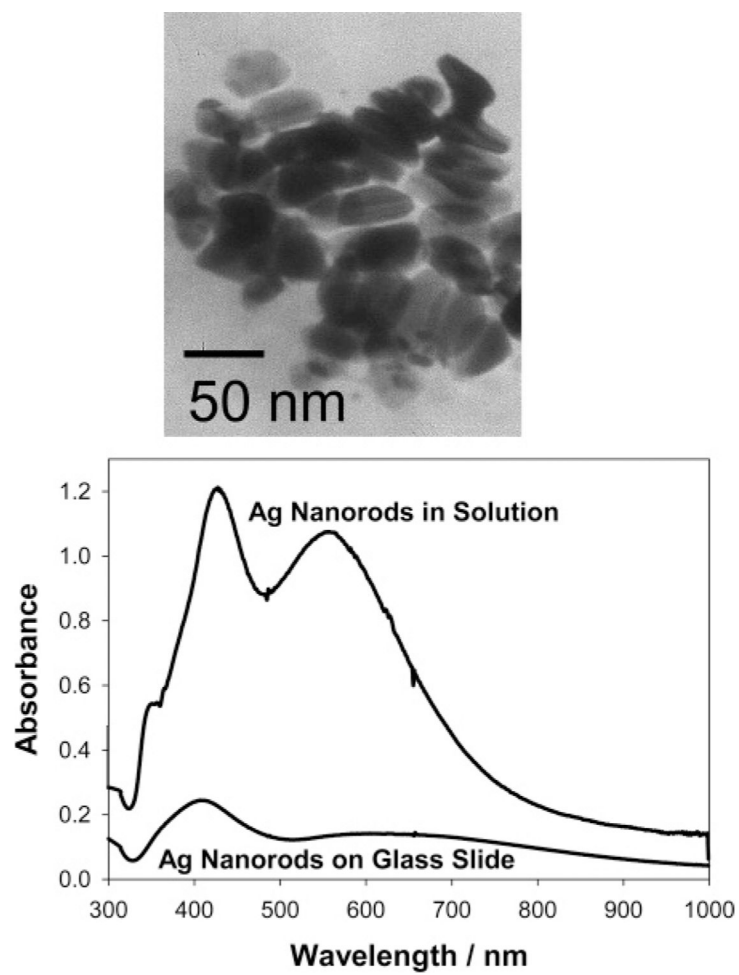


Figure 2. TEM image of silver nanorods grown in solution (top) and absorption spectra of silver nanorods deposited on glass substrates by slow deposition (bottom).

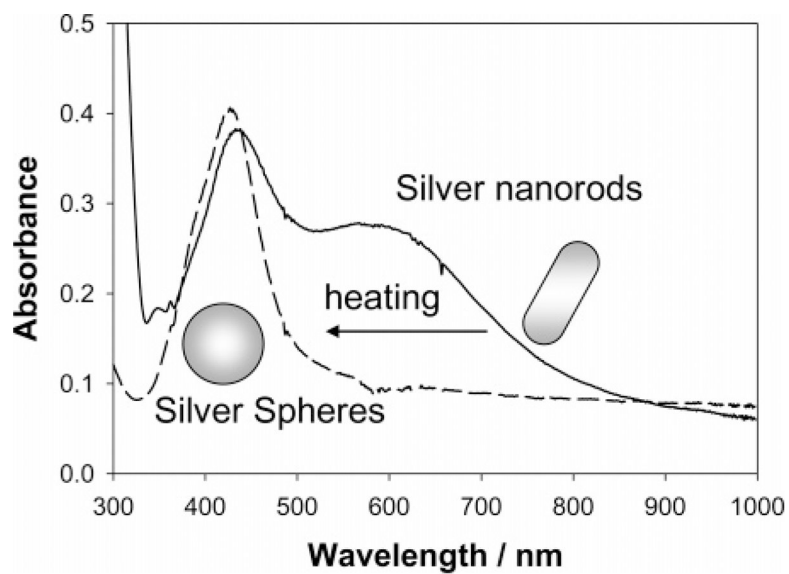


Figure 3. Absorption spectra of silver nanorods in growth medium before and after continuous heating at 40 °C for 48 h.

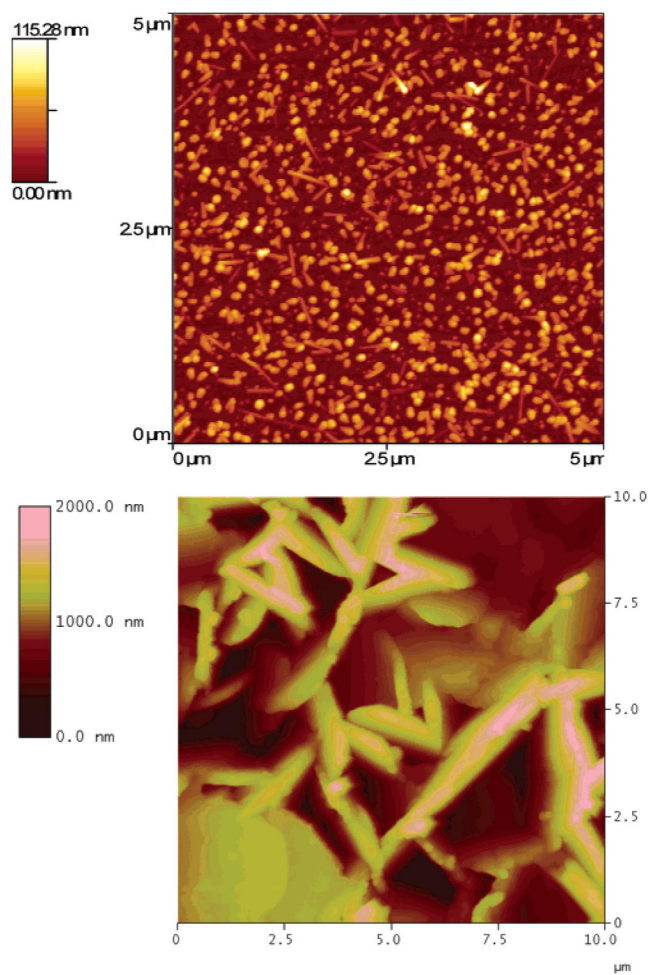


Figure 4. AFM images of silver nanorods with low loading density (top) and with high loading density on glass substrates (bottom).

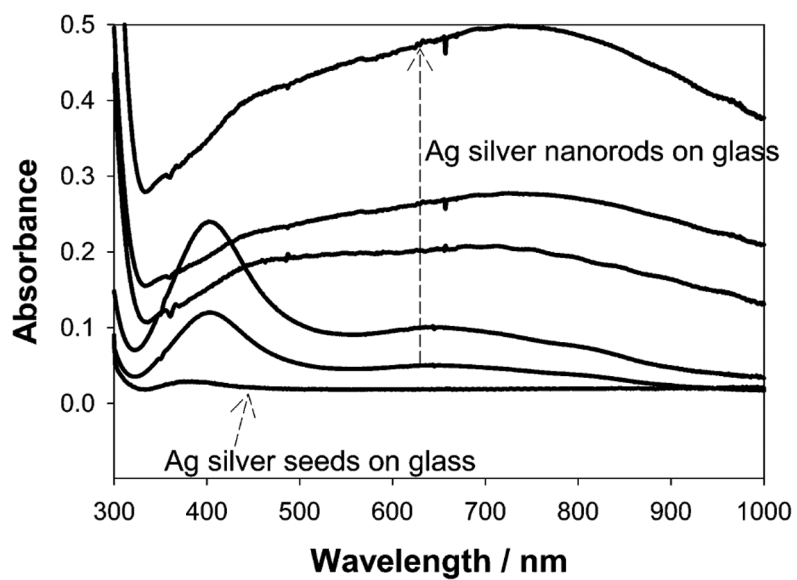


Figure 5. Absorption spectra of silver seeds and silver nanorods deposited on glass substrates by rapid deposition.

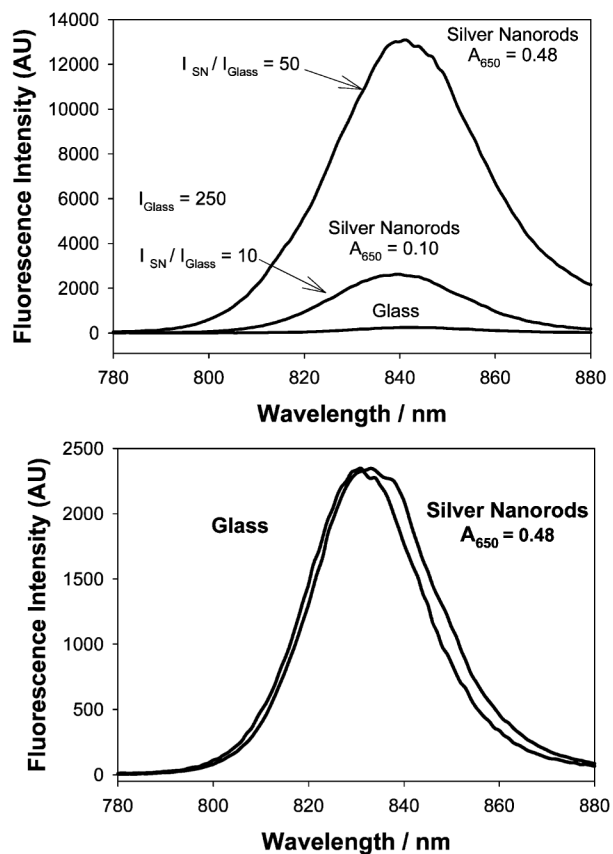


Figure 6. Fluorescence emission intensity of ICG-HSA on silver nanorods with low ($A_{650} = 0.10$) and high ($A_{650} = 0.48$) loading density (top). The arbitrary emission intensity of ICG-HSA on glass is 250. Normalized emission intensities of ICG-HSA on glass and on silver nanorods ($A_{650} = 0.48$), showing identical spectral behavior (bottom).